Dean&Francis

ISSN 2959-6157

Compliant Control System for Throat Swab Sampling

Qi Liu

School of Wuyi University,
Dongguan, Guangdong, China
Email: lq2462395251@163.com

Abstract:

In contemporary medical conditions, we can see medical robots in many medical places. For example, in modern surgery, it is not difficult to learn that the cutting-edge robot-assisted minimally invasive technology has more and more applications to replace the traditional open surgery. For example, cardiac luminal intervention, colonoscopy, vascular intervention and so on. The existence of these assisted robots greatly improves the success rate of surgery. Since a medical robot can perform minimally invasive surgery, it can also be competent for sampling viruses in daily life. In this paper, we will summarize the control mode of virus sampling robot in the past, and propose a robot with flexible linear control, which can realize more accurate positioning and sampling of virus sampling on patients, so as to realize the accuracy and efficiency in the sampling process.

Keywords: Medical, robotic, assisted, viral, compliant and linear control

1. Introduction

The sudden outbreak of the COVID-19 pandemic has brought significant changes to people's lives, as well as a tremendous impact on various fields, especially healthcare services. The respiratory swab virus testing technology is characterized by high accuracy and simplicity in operation, making regular virus testing a key measure in epidemic prevention and control [1]. Currently, there is relatively little research on virus sampling robots both domestically and internationally, compounded by the uniqueness of their usage scenarios. This has slowed down the development and research process of virus sampling robots. This study focuses on the UR10e robotic arm equipped with a six-dimensional force sensor and a passive compliance structure composed of dual linear springs, coupled with a multi-point force sensing system made of carbon fiber and an active compliance control system, forming a hybrid passive-active compliance (APC) robot. The APC robot features finer and more sensitive force feedback and control systems, and it offers more controllable and precise spatial positioning of the swab tip, thereby enabling compliant and safe sampling operations. This paper studies a robot that uses the UR10e robotic arm as its motion structure, equipped with a passive compliance structure at its front end formed by dual linear springs, creating a hybrid passive-active compliance robot that includes a multi-point force sensing system made from carbon fiber and an active compliance control system. The robot is designed to provide finer and more sensitive force feedback and control, as well as easier control

and clearer spatial positioning of the swab tip, facilitating compliant and secure sampling operations.

2. Literature Review

Passive compliance control relies on the physical compliance of certain mechanical devices to adapt passively to contact forces. Compliance devices composed of springs, dampers, and similar components can absorb or dissipate the energy generated during contact between the robot and its environment through spring deformation or damping losses. Based on this compliance control concept, researchers in various countries have designed multiple compliance devices. For instance, an elastic component can be applied in the joint transmission chain of a robot to form a series elastic actuator [2-3]. However, this brings about the consequence of reduced structural stiffness, which in turn affects the precision of motion control. To balance the compliance performance of collaborative robots and positional accuracy, increasing the use of specially designed variable stiffness devices in drive joints has emerged as a new research hotspot. Representative works include the variable stiffness actuator developed by Tonietti [4], the variable stiffness joint developed by the German Aerospace Center [5], and the variable stiffness actuators developed by Professor Darwin G. Caldwell and colleagues[6-8] at the Polytechnic University of Milan. Although these structures can alter joint stiffness to varying degrees, they significantly increase the weight, structural complexity, and control difficulty of the joints, and they are still in the research and development phase with limited practical application in collaborative robots. Currently, commonly used active compliance control generally falls into two categories: force/position hybrid control and impedance control.

Force/position hybrid control for robotic arms was initially proposed by Raibert and Craig [9], also known as RC control. This system includes position and force feedback loops, requiring real-time feedback of the robotic arm's current position and the environmental forces detected by force sensors, enabling direct control of the interaction forces between the robotic arm's end effector and the environment [10]. In stark contrast to force/position hybrid control, impedance control considers force and position control together within a control space. Nagata and others [11] designed a contact surface-based position/force impedance controller, which stabilizes force control by adjusting the force control loop through the position control loop. He and others[12] proposed a force-tracking dual-variable stiffness dual impedance control method for cooperative robots interacting with objects in a shared environment, allowing the control system to exhibit adaptive characteristics in both external and internal forces, effectively tracking both position and force. Professor Darwin G. Caldwell and others [13] explored an impedance control method that replaces the force control loop with a velocity PI control loop, which offers advantages of easy parameter adjustment, good robustness, and effective friction force compensation. Stefan and others [14] combined impedance control, admittance control, and expectation-based force control into a single architecture, ensuring that the robot's compliance control maintains good stability and control performance even near singular points, where the impedance parameters influence the changes in contact forces between the robot and the environment, as well as the trajectory tracking performance.

3.Simulation Experiments

3.1 Simulation Experiments

3.1.1 Technical Route

ISSN 2959-6157

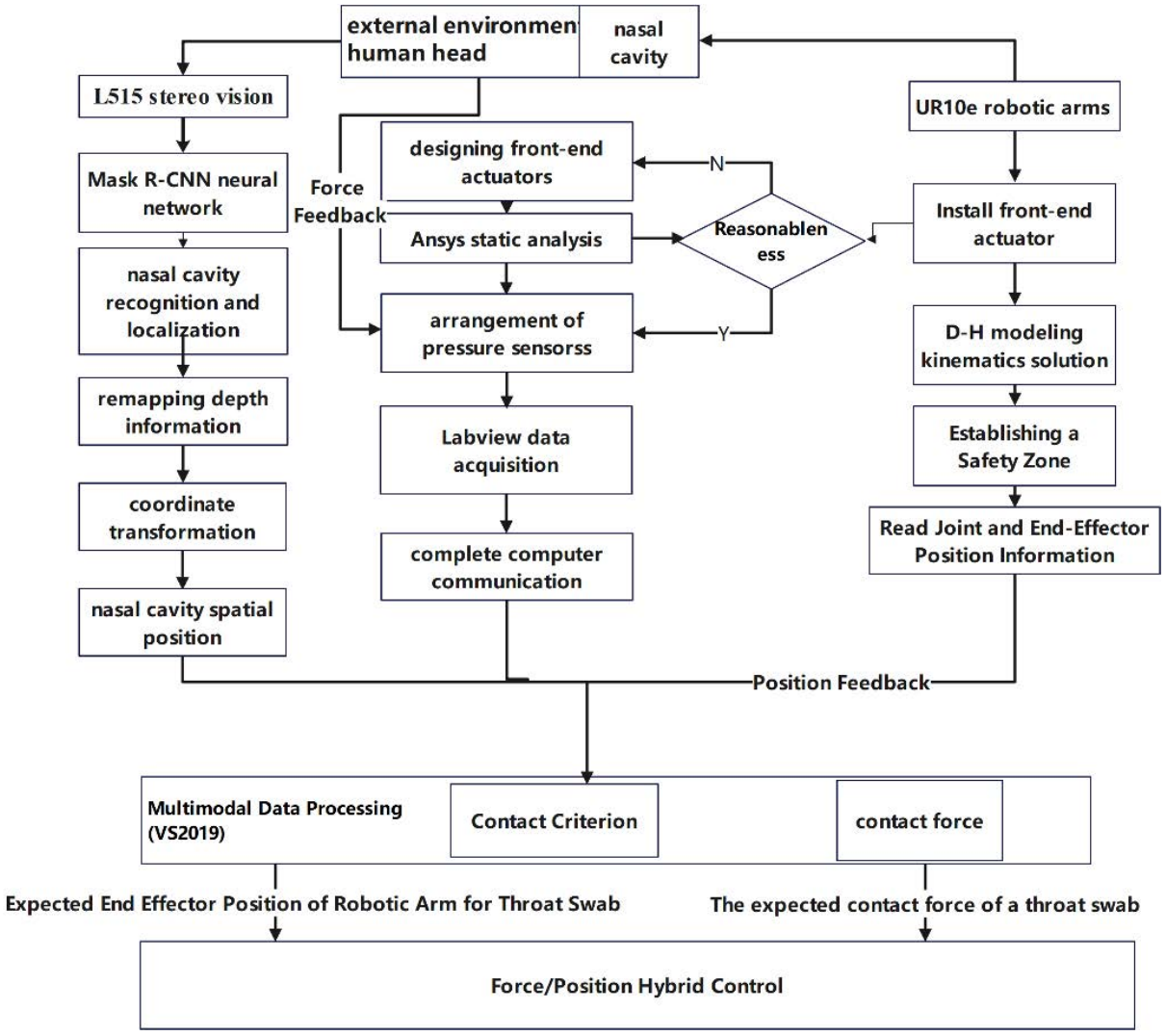

Figure 1 Technical Route Diagram

First, we design and select components and materials based on the force sensor to achieve the design of a one-dimensional force sensor. Building on the one-dimensional force sensor, we then design a multi-dimensional force sensor, followed by testing and modifications to finalize the design scheme. Next, we will arrange the six-dimensional force sensor at the end position of the actuator.

3.1.2 Implementation of Compliant Control

(1) Use the L515 laser camera to capture images of the detection position;

(2) Perform image recognition to obtain the spatial position of the oral cavity's center point;

(3) Drive the robot to move in free space, during which Fd=0 and Fe=0 until reaching the target position at the center of the oral cavity;

(4) Slowly advance the robot arm on the X-axis.When Fe>0,the robot arm immediately stops moving to obtain the equilibrium position Xe;

(5) Use Fd as the desired sampling force and Xe as the equilibrium position to perform admittance control for constant force adjustment, while conducting upward and downward rotational sampling;

(6) After completing the sampling action, the APC robot is retracted.

Combining passive compliant kinematics, force feedback, and visual recognition of the target position, the system's admittance control transfer function is designed as shown in Figure 2.

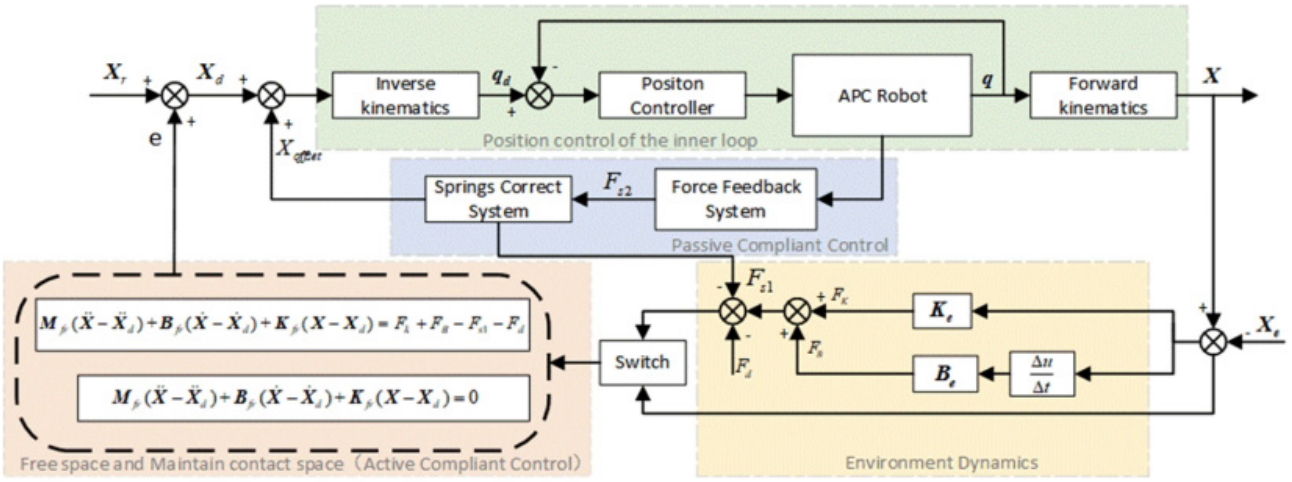

FFigure 2 Robot Compliant Control Design

3.1.3 Implementation of Communication and Machine Recognition

The robotic arm communicates with the computer via a local area network (LAN) through a switch, completing bidirectional communication for robotic arm status acquisition and control. The vision system transmits image data and depth information to the computer through a USB3.2 interface. The force feedback system communicates with the computer via a USB 2.0 interface. This completes the system setup for subsequent research on compliant control technology.

1) First Layer Recognition Processing: Search for image features, match facial features, and segment the facial ROI (Region of Interest).

2) Second Layer Recognition Processing: Search for mouth features within the facial ROI, typically characterized by brightness, with the sides darker and the center brighter. Extract and segment the mouth ROI, and perform morphological processing to obtain a binary image. Apply Canny edge detection to the binary image to extract contour corner points, perform quadrant filtering on the corner points, and search for the maximum inscribed circle to obtain the pixel coordinates of the mouth center.

3.1.4 Camera Parameter Calibration

To avoid image recognition errors caused by environmental factors such as lighting, a 3D point cloud visual recognition system composed of LiDAR laser cameras is used, providing a more accurate target position in the oral cavity. The scene setup is shown in Figure 3.

Figure 3 Simulated Scene Effect Diagram

ISSN 2959-6157

Using Visual Studio 2019, the development environment required for the Mask R-CNN neural network is set up. The L515 monocular vision camera is employed to locate the nostrils of the detected individuals and obtain planar coordinates. After obtaining the target pixel coordinates, we need to calibrate the camera to acquire its intrinsic and extrinsic parameters. These parameters will be used to convert the pixel coordinates into camera coordinates. Subsequently, the hand-eye calibration method is applied to calculate the transformation matrix from the camera center to the tip of the swab, referred to as the hand-eye matrix; the formulas are not presented here.

Using MATLAB, a chessboard image of size 15 mm × 15 mm is utilized as a calibration reference to obtain accurate camera distortion parameters. By using 15 different images of the calibration board placed at random angles, corner points of the chessboard images can be successfully identified, resulting in the camera's intrinsic and extrinsic parameters, the pose of the calibration images, and the re-projection error. The local 3D view of the camera module, calibration images from various angles, and the camera's intrinsic and extrinsic parameters are illustrated in Figures 4 to 7.

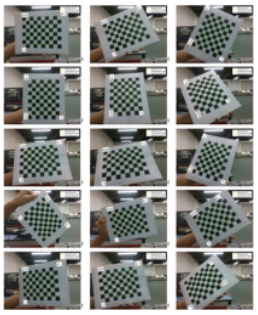

Figure 4 (Left)Local 3D View of the Camera Module for theImplementation Plan

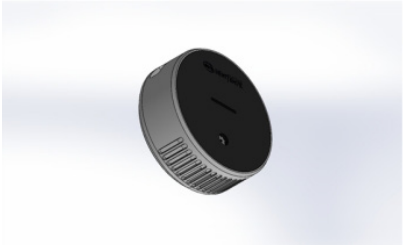

Figure 5 (Right)Calibration Images from Different Angles

intrinColor	{width=640 height=480 ppx=330.192413 ...}	rs2_intrinsics
width	640	int
height	480	int
ppx	330.192413	float
ppy	240.773041	float
fx	601.960693	float
fy	601.895020	float
model	RS2_DISTORTION_BROWN_CONRADY (4)	rs2_distortion
coeffs	0x000000b90efedcd4 {0.156788841, -0.488065869, -0.00196838332, 0.000321554689, 0.456559360}	float[5]
[0]	0.156788841	float
[1]	-0.488065869	float
[2]	-0.00196838332	float
[3]	0.000321554689	float
[4]	0.456559360	float

Figure 6 Camera Intrinsic Parameters

extrinDepth2Color	{rotation=0x000000b90efedd08 {0.999952435, -0.00959051866, -0.00178425759, 0.00951919425, 0...	rs2_extrinsics
rotation	0x000000b90efedd08 {0.999952435, -0.00959051866, -0.00178425759, 0.00951919425, 0.99929130...	float[9]
[0]	0.999952435	float
[1]	-0.00959051866	float
[2]	-0.00178425759	float
[3]	0.00951919425	float
[4]	0.999291301	float
[5]	-0.0364186056	float
[6]	0.00213226629	float
[7]	0.0363998897	float
[8]	0.999335051	float
translation	0x000000b90efedd2c {-0.00161810499, 0.0139144920, -0.00136217114}	float[3]
[0]	-0.00161810499	float
[1]	0.0139144920	float
[2]	-0.00136217114	float

Figure 7 Camera Extrinsic Parameters

Finally, a 1:1 model of the human head is used for nucleic acid sampling tests and validations. The analysis examines the impact of the contact force between the robotic arm and the human nasal cavity on the results of nucleic acid sampling. Additionally, a staining method is employed to verify the effectiveness of the sampling. Based on the results, adjustments and optimizations are made to the force/position hybrid control of the robotic arm. The robotic arm's entry into the nasal cavity during the experiment is illustrated in Figure 8.

Figure 8 Experiment of the Robotic Arm Entering the Nasal Cavity

4. Conclusion

This study focuses on the UR10e robotic arm equipped with a six-dimensional wrist force sensor, exploring a Active-Passive Compliance (APC) robot. The robot features a passive compliant structure composed of bi-linear springs, combined with a multi-point force sensing system made from carbon fiber wires and an active compliance control system. The APC robot offers finer and more sensitive force feedback and control capabilities, enabling easier control and clearer spatial positioning of the swab tip, resulting in compliant and safe sampling operations.

By utilizing the six-dimensional wrist force sensor for force feedback, we designed and validated an impedance controller based on force-position feedback, and investigated the characteristics of impedance parameters. During the nucleic acid sampling process, we leveraged both visual and tactile feedback, employing a compliant structure to achieve adaptability in the sampling procedure. This effectively addresses the issues of low positional accuracy and poor controllability in passive compliant structures under force. This research contributes significant practical value and broad application scenarios for medical auxiliary diagnosis, advancing the application of related technologies in the healthcare field.

References

[1]. Gu, B. (2021). COVID-19 Detection Technologies and Clinical Research Strategies. *Chinese Journal of Clinical Laboratory Management*, 9(3), 192.

[2]. R.D.Howard. Joint and actuator design for enhance dstability in robotic control [D] . Massachusetts Institute of Technology,Cambridge,MA,USA,1990.

[3]. A. Calanca and P.Fiorini.On the roleof compliance in force control[C].Int. Conf . intelligent Autonomous Systems,2014.

[4]. Tonietti G,Schiavi R and Bicchi A .Design and Control of a Variable Stiffness Actuator for Safe and Fast Physical Human / Robot Interaction[C].IEEE International Conference on Robotics and Automation,2005:526-531.

[5]. FF lacco and ADE Luca . A pure signal - based stiffness estimation for VSA devices[C].IEEE International Conference on Robotics and Automation ,2014:2418-2423.

[6]. Jafari A ,Tsagarakis NG and Caldwell DG .Aw AS-II :A new Actuator with Adjustable Stiffness based on the novel principle of adaptable pivot point and variable lever ratio [C]. IEEE International Conference on Robotics and Automation ,2011:4638-4643.

[7]. Tsagarakis NG,Sardellitti I and ald well DG.Anew variable stiffness actuator (CompAct-VSA) : Design and modelling [C] .IEEE International Conference on Intelligent Robots and Systems,2011:78-383

[8]. AJafari, NGT sagarakis and DGC aldwell .A Novel Intrinsically Energy Efficient Actuator With Adjustable Stiffness

ISSN 2959-6157

(AwAS) [C]. IEEET ransactions on Mechatronics , 2013:355-365.

[9]. Udai AD ,Saha SK.Dynamic simulation of serial robots under force control [J].International Journal of Intelligent Machines and Robotics, 2018 , 1(1):79-108.

[10]. Wei L,Li E, Wang H.Hybrid force /position control based on mixed optimal neural networks [J]. Electric Machines and Control,2006,10(2):151.

[11]. F.Nagata, T.Hase, Z. Haga, eta l.CAD/CAM-basedposition /force controller for am old polishing robot[J]. Mechatronics,2007,17:207-216.

[12]. J.He, M.Luo and Q. Zhang. Dual impedance control with variable object stiffness for the dual -arm cooperative manipulators [C]. Asia-Pacific Conference on Intelligent Robot Systems , 2016 : 102-108.

[13]. Mosadeghz ad M, Medrano-Cerda GA,Saglia JA,eta l.Comparison of various active impedance control approaches, modeling,implementation,passivity,stability and trade-offs[C]. IEEE/ASME International Conference on Advanced Intelligent Mechatronics.2012.

[14]. Stefan S,Arne R and Rudiger D,Forward Dynamics Compliance Control (FDCC) :A New Approach to Cartesian Compliance for Robotic Manipulators [C].IEEE/RSJ International Conference on Intelligent Robots and Systems,2017.